Impact of Power Control Optimization on the System Performance of Relay Based LTE-Advanced Heterogeneous Networks

Ömer Bulakci, Simone Redana, Bernhard Raaf, and Jyri Hämäläinen

Abstract: **Decode-and-forward relaying is a promising enhancement to existing radio access networks and is already standardized in 3rd generation partnership project (3GPP) as a part of long term evolution (LTE)-Advanced Release 10. Two inband operation modes of relay nodes are supported, namely type 1 and type 1b. Relay nodes promise to offer considerable gain for system capacity or coverage, depending on the deployment prioritization, in a cost-efficient way. Yet, in order to fully exploit the benefits of relaying, the inter-cell interference which is increased due to the presence of relay nodes should be limited. Moreover, large differences in the received power levels from different users should be avoided. The goal is to keep the receiver dynamic range low in order to retain the orthogonality of the single carrier-frequency division multiple access system. In this paper, an evaluation of the relay based heterogeneous deployment within the LTE-Advanced uplink framework is carried out by applying the standardized LTE Release 8 power control scheme both at evolved node B and relay nodes. In order to enhance the overall system performance, different power control optimization strategies are proposed for 3GPP urban and suburban scenarios. A comparison between type 1 and type 1b relay nodes is as well presented to study the effect of the relaying overhead on the system performance in inband relay deployments. Comprehensive system level simulations show that the power control is a crucial means to increase the cell edge and system capacities, to mitigate inter-cell interference and to adjust the receiver dynamic range for both relay node types.**

Index Terms: **Inband relay, long term evolution (LTE)-Advanced, performance evaluation, power control (PC), uplink.**

I. INTRODUCTION

The universal mobile telecommunications system (UTRAN) long term evolution (LTE) is being designed to enhance 3rd generation (3G) radio access technologies and it represents a major step towards the international mobile telecommunications (IMT)-Advanced technologies of the international telecommunication union-radiocommunications sector (ITU-R). The IMT-Advanced radio access technologies are expected to offer increased broadband capacity with high quality of service for next generation multimedia services, such as, high-definition

TV content, video chat, mobile TV, and real-time gaming. Requirements for the IMT-Advanced technologies are defined by ITU-R in a circular letter issued in March 2008 calling for candidate radio access technologies [1].

In response to ITU-R circular letter, 3rd generation partnership project (3GPP) made a formal submission in September 2009 proposing LTE Release 10 (Rel. 10) and beyond as a candidate IMT-Advanced technology [2]. The proposed radio access technology is referred to as LTE-Advanced and is expected to meet and even exceed the IMT-Advanced requirements [3]. LTE-Advanced utilizes single carrier-frequency division multiple access (SC-FDMA) and orthogonal frequency division multiple access (OFDMA) as the uplink and downlink transmission schemes, respectively. Both of these schemes employ orthogonal radio resources and thus impose ideally no intra-cell interference which is typical for code division multiple access (CDMA) based systems such as wideband CDMA (WCDMA) and high speed packet access (HSPA).

To address the stringent requirements of IMT-Advanced, different key technologies have been investigated in the 3GPP study item on LTE-Advanced, of which bandwidth extension via carrier aggregation, improved multiple-input multiple-output (MIMO) schemes, coordinated multi-point transmission and reception, and heterogeneous deployments comprising low-power nodes like femtocells and decode-and-forward relay nodes (RNs) [4], [5]. In this paper, we focus on decode-and-forward RNs as a major technology enhancement.

RNs are specified in the 3GPP work item on LTE-Advanced networks to meet the growing demand and challenging requirements for coverage extension and capacity enhancement [5]. RNs are relatively small nodes with low power consumption, which connect to the core network with wireless backhaul through an evolved node B (eNB), referred to as the donor eNB in 3GPP terminology. The wireless backhaul enables deployment flexibility and eliminates the high costs of a fixed backhaul. Thanks to the compact physical characteristics and low power consumption, RNs can be mounted on structures like lamp posts with power supply facilities. Furthermore, RNs do not have strict installation guidelines with respect to radiation, visual disturbance and planning regulation. Therefore, installing RNs involves lower operational expenditure [6] and faster network upgrade when operators aim to improve the quality of service [7]. Previous studies have further shown that RNs promise to increase the network capacity [8]–[10] and to better distribute resources in the cell, or alternatively, extend the cell coverage area [9]–[12].

In 3GPP, three RN types are specified according to the ap-

plied spectrum usage approaches on the wireless backhaul link between RN and its donor eNB. Type 1 and type 1b are inband RNs where the same spectrum is used for both the relay backhaul and the access link between RNs and the served user equipments (UEs), whereas type 1a is an outband RN which uses a different spectrum for the relay backhaul. We note that, as the relay (eNB-RN) and access (RN-UE) links are time-division multiplexed in the inband approach, operating both links on a single carrier frequency may eliminate the need for additional licensed spectrum [5]. Considering the scarcity of available spectrums and the high costs of licensed ones, type 1b RNs aim to increase the performance by introducing enough isolation between the antennas used for the access and relay links, e.g., by means of well separated and well isolated antenna structures. This will allow simultaneous operation of both links and thus relaxes the relay link. All these relay types control their own cells, i.e., they have their own physical cell identifications (IDs) and include functionalities such as radio resource management, scheduling and hybrid automatic repeat request retransmission control.

Relay deployments will require a more detailed dimensioning and planning than conventional single-hop networks. RN-served UEs (relay-UEs) can create severe inter-cell interference in particular when a large number of RNs are deployed in the cell with a reuse factor of one. Consequently, power control (PC) becomes an important means in the uplink transmission of relay cells not only to compensate for channel variations, but also to mitigate the interference and to increase the cell edge and system capacities. Moreover, PC can ensure that the receiver dynamic range does not exceed a certain level by decreasing the difference between received power levels of different nodes in the same cell. A high receiver dynamic range increases the susceptibility of SC-FDMA (a.k.a., discrete Fourier transform spread-orthogonal frequency division multiplexing (OFDM)) to the loss of orthogonality and hence can cause intra-cell interference [13]. Besides, in contrast to homogeneous (eNB-only) networks, a proper PC is as well necessary for the relay link because the end-to-end throughput (TP) experienced by relay-UEs depends on the qualities of both the access and relay links. We note that in the following discussion the mentioned end-to-end link contains the link from eNB to RN and the link from RN to UE.

PC has been analyzed in numerous studies and many fundamental works were published during 90's when CDMA development was ongoing, see e.g., [14] and [15]. From LTE perspective, important extension to classical works was introduced in [16] where the idea of fractional PC (FPC) was analytically investigated for the first time. The LTE uplink PC is built on FPC and [16] provides a good starting point for analytical studies on LTE PC parameter optimization. Like shown also in [17], such investigations may present in an elegant way relations between parameters and also provide guidelines for practical algorithm design. Nevertheless, for credible system level performance evaluation of practical network deployments extensive multi-cell simulations are needed in order to produce statistics for key performance indicators that rely on TP distributions. Within the single-hop LTE Rel. 8 framework such simulation based performance evaluation of PC has been well elaborated in the literature [18]–[22]; however, for LTE-Advanced

relay deployments PC parameter optimization problems are not yet widely examined. We recall that in our initial study [23] it was shown that LTE Rel. 8 compliant PC is as well appropriate for relay based heterogeneous networks and applying a heuristic optimization methodology we have presented an increase in the system performance. In another study [24], the PC optimization is done according to the imposed interference proportions and we have shown that for the maximum performance enhancement, PC parameters should be optimized not only at the RNs but also at the eNBs. In these studies, the PC optimization was carried out in urban scenarios for direct (eNB-UE) and access links only and the relaying overhead was neglected.

In this paper, an evaluation of the relay based heterogeneous deployment within the LTE-Advanced uplink framework is carried out by applying the standardized LTE Rel. 8 PC scheme both at eNBs and RNs. In order to enhance overall system performance, different power control optimization strategies are proposed for 3GPP urban and suburban scenarios. We carry out comparisons against two main reference cases. *First, we benchmark the performance gain from type 1 relays against single-hop homogeneous deployment where relays are not deployed at all*. Although this comparison is not topologically fair, it provides understanding about the return for the relaying investment. *Second, we use ideal type 1b relays as a reference*. We note that here the term '*ideal*' refers to the fact that for reference type 1b relays the impact of relay link is ignored. In this case, the comparison is fair from network topology perspective but obviously, half-duplex type 1 relay performance cannot exceed the performance of ideal type 1b relays. Instead, we aim to show that losses due to half-duplex relaying become marginal especially in coverage-aimed scenarios. Thus, type 1 relays represent a cost-effective alternative for type 1b relays which usually require costly antenna arrangements. Thorough system level simulations that follow the most recent 3GPP guidelines are conducted within the LTE-Advanced framework to examine the system performance of relay deployments.

The remainder of the paper is organized as follows. Section II provides the background material including PC, key features of the general framework and the definitions that are utilized throughout the paper. In Section III the system model and simulation assumptions along with the multi-hop relay scenario are given. In Section IV detailed performance evaluation and analysis are carried out. The paper is concluded in Section V.

II. BACKGROUND AND DEFINITIONS

In this section, we first recall the framework of LTE uplink technology. Then, FPC scheme of LTE Rel. 8 is outlined. The key features of the work and the definitions are presented next.

A. LTE Uplink Technology

LTE uplink has adopted SC-FDMA [25] due to its low peak-to-average power ratio allowing low power consumption and high efficiency at the UE. This property is particularly important for UE battery lifetime. The total bandwidth available for the uplink transmission is defined by the multiplexing scheme used. In our work, we assume frequency-division duplex (FDD) to separate uplink and downlink transmissions. In the fre-

quency domain, the whole uplink bandwidth is divided into sub-bands which are called physical resource blocks (PRBs). The PRB defines the resource allocation granularity in LTE. For instance, when the system is operating on 10 MHz bandwidth there are $M_{total} = 48$ PRBs available for data transmission on the physical uplink shared channel (PUSCH) and 2 PRBs are reserved to the physical uplink control channel (PUCCH). The main difference of SC-FDMA compared to OFDMA is the single-carrier constraint, where only a set of adjacent PRBs can be allocated to a UE. Such a constraint impacts the frequency domain scheduler and imposes a trade-off between multi-user diversity and the bandwidth utilization. In the time domain, users can be scheduled to a subset of M_{total} PRBs in each transmission time interval (TTI). A TTI (a.k.a., subframe) duration is 1 ms and an LTE frame consists of 10 subframes.

B. Power Control

Thanks to the orthogonality of SC-FDMA, intra-cell interference is not of main concern in LTE. The aim of PC mechanisms is then to maximize the received power of wanted signals through compensating the long-term channel variations, while limiting the amount of the inter-cell interference generated. We note that the term PC is used in LTE uplink, although especially the open-loop PC is more like a power allocation in nature. However, in LTE the term power allocation is reserved for downlink and in order to avoid confusion we have followed the terminology defined in LTE standards [26].

Nevertheless, the receiver dynamic range[1] of eNBs and RNs should also be adjusted via PC to avoid intra-cell interference, where a high dynamic range can cause the loss of orthogonality. To fulfill these objectives, in LTE, FPC for the PUSCH is used to determine the UE transmit power [26]. In this work, FPC is also employed for the relay specific PUSCH which is the physical channel for the uplink relay link data transmission. Accordingly, the transmit power of a node u (UE or RN) is given in dBm as

$$P_u = \min\{P_{max}, P_0 + 10\log_{10} M_u + \alpha L + \Delta_{TF}(i) + f(i)\}. \tag{1}$$

In this equation,

- P_{max} is the maximum allowed transmit power (a.k.a., power headroom), which has an upper limit of 23 dBm for UE power class 3 [27] and 30 dBm for RN transmissions (optionally 37 dBm for suburban scenarios) [5],
- P_0 is the power offset comprising cell-specific and node specific components and it is used for controlling the received signal-to-noise-ratio (SNR) target that can be set from -126 dBm to P_{max} with a step size of 1 dB,
- M_u is the number of PRBs allocated to node u,
- α is a 3-bit cell-specific path loss compensation factor that can be set to 0.0 and from 0.4 to 1.0 with a step size of 0.1,
- L is the downlink path loss estimate calculated by the node,
- $\Delta_{TF}(i)$ and $f(i)$ are the node specific closed-loop correction and the modulation and coding scheme (MCS) offset, respectively. Note that, these parameters are optional.

[1] The receiver dynamic range is defined as the difference in dB between the 5th%-ile and 95th%-ile of the cumulative distribution function (CDF) of the total received power.

Since SC-FDMA does not suffer from either intra-cell interference or near-far effects and the cell-specific parameters have the main impact on the inter-cell interference, the latter optional closed-loop parameters in (1) are not considered decisive and hence excluded. In addition, omitting these parameters is advantageous in the sense that it saves the overhead due to signaling especially when a large number of users are served in a cell. Besides, in [19] the performances of open-loop PC and signal-to-interference-plus-noise-ratio (SINR)-balancing closed-loop PC were compared. Therein, it was shown that closed-loop PC performs poorly at high load relative to open-loop PC, as closed-loop PC does not utilize the link adaptation and cannot fully exploit the link performance capability in LTE. This work focuses on evaluating the performance of open-loop PC.

Open-loop PC compensates slow channel variations, i.e., path loss changes including shadowing, while limiting the inter-cell interference. If α is set to one in (1), the path loss is fully compensated and the resulting scheme is called full compensation PC (FCPC). For a given P_0 value, FCPC improves the cell-edge user performance at the cost of increased inter-cell interference due to higher transmit power levels. Yet, the inter-cell interference can be reduced by setting α smaller than one, which increases the cell-center performance, however, at the cost of penalizing the cell-edge performance [18], [19]. One of the important determinants of the motivation of studying the applicability of the existing FPC for the relay enhanced cells is the desired backward compatibility between LTE Rel. 8 and LTE-Advanced terminals, i.e., the legacy LTE Rel. 8 terminals which cannot be updated with a new PC scheme should also support relay operations. Thus, the derivation of the optimal parameter setting of the existing PC for the relay scenario is needed.

Regarding to performance evaluation methodology, we note that even in pure slow fading model (fast fading ignored) the system level performance of open-loop PC (1) is difficult to quantify analytically. Namely, if interference is ignored, then distribution of received SNR in decibel scale can be easily computed since L in (1) is Gaussian. Yet, the impact of inter-cell interference is of main interest but if it is considered, then simplifications/approximations are needed since interference terms include sums of lognormal variables with different parameters. Furthermore, relay deployment impacts to the spatial distribution of interferers and we should take into account the handover to the best cell, which may be a relay cell, before applying PC. Thus, brute force simulations seem to be the only way to obtain practically feasible results when 3GPP performance indicators are used.

C. PDCCH Limitation

As previously mentioned, due to single-carrier constraint in uplink the number of scheduled UEs per TTI should be high to take advantage of the frequency selectivity of the channel. However, in practice the maximum number of the UEs that can be scheduled in each TTI is limited by the possible number of scheduling grants which are carried by the physical downlink control channel (PDCCH). A scheduling grant includes dedicated user information which is necessary to decode the data channel, e.g., data bandwidth allocation and MCS. Typically 8–10 UEs can be scheduled per TTI because of PDCCH limi-

tation (or PDCCH blocking) [28]. In this work, this number is set to 8. That is, if there are more than 8 UEs accessing to an access node, a subset consisting of 8 UEs will be scheduled in each TTI. The unscheduled UEs in a given TTI will be scheduled in other TTIs in a way that resource fairness is achieved in the time domain. Note that in reality PDCCH limitation changes from TTI to TTI depending on the used control channel elements by the served UEs. A cell-center user with better channel conditions requires less number of control channel elements, whereas this number increases as the channel conditions worsen towards the cell edge [29]. We further note that we assume that, in the considered relay scenario, there is no limitation on the relay specific PDCCH as the relay link experiences good channel conditions and does not suffer from severe fast fading because RNs are deployed at fixed locations.

D. Power Limitation and Adaptive Transmission Bandwidth

The maximum number of PRBs—denoted by $M_{\mathrm{max,u}}$—which can be assigned to a UE depends on the difference between P_{max} and the per-PRB power spectral density (PSD) of that UE. The per-PRB PSD of a UE can be obtained via the open-loop component of (1) by setting $M_u = 1$ such that

$$\mathrm{PSD}_u = \min\{P_{\mathrm{max}}, P_0 + \alpha L\}. \tag{2}$$

Thus, PSD is simply the transmit power per PRB. Note that the actual PSD is given by (2) as long as the UE is not driven into power limitation, otherwise P_{max} will be equivalently spread over the assigned PRBs resulting in decreased SINR per PRB. Such an assignment may result in outage especially when the UE is experiencing poor channel conditions. Consequently, $M_{\mathrm{max,u}}$ is obtained as

$$M_{\mathrm{max},u} = \mathrm{round}\left(10^{0.1(P_{\mathrm{max}} - \mathrm{PSD}_u)}\right) \tag{3}$$

where round (x) is the smallest integer not less than x.

Hence, power-limited UEs will not be assigned to more resources than those they can afford, and the unused resources can be better utilized by other users resulting in more efficient bandwidth usage. This functionality is called adaptive transmission bandwidth [30]. It is worth mentioning that in contrast to [30] where *floor* operator is used, we have adopted *round* operator. The aim is to decrease the quantization errors caused by this operation and to further enhance the performance over the P_0 set of interest. It is as well empirically justified via our simulations. A detailed comparison of adaptive transmission bandwidth with fixed transmission bandwidth is given in [31]. Therein, it is shown that adaptive transmission bandwidth is particularly advantageous for suburban scenarios having large inter-site distances (ISDs).

E. Performance Metrics

Throughout the paper, the following key performance metrics are used.

- 5%-ile user TP: The 5%-ile user TP level of cumulative distribution function (CDF) is multiplied by the average number of users per sector. This metric reflects the cell-edge bitrate or equivalently the cell coverage performance.

- Cell capacity: Aggregate user TP per sector.
- 50%-ile user TP: The 50%-ile user TP level of CDF is multiplied by the average number of users per sector. This metric gives an intuition about the mean user TP.
- Geometry (wideband SINR): In 3GPP lingo, the geometry of a node (UE or RN) is determined without considering the impact of scheduling on the downlink, i.e., wideband SINR is calculated in dB as

$$G_{\mathrm{SINR}} = \frac{P_w}{\sum_n P_{i,n} + P_N} \tag{4}$$

where P_w is the received wanted signal power, $P_{i,n}$ is the interference power imposed by the nth interfering node and P_N is the thermal noise power over the considered bandwidth. Moreover, transmit or receive diversity gains due to MIMO techniques are not included. The geometry metric is of particular interest for analyzing different implementations, e.g., installation of directional antennas at access nodes.

III. SYSTEM MODEL

This section describes essential features of the system model such as the considered relay scenario along with the applied resource sharing techniques and the channel models that pertain to the propagation scenarios. The simulation parameters complying with the latest 3GPP guidelines within the LTE-Advanced framework [5] are given at the end of the section.

A. Multi-Hop Relay Scenario

RNs will be deployed by operators in contrary to, e.g., femtocells for which random deployment by subscribers may take place. Considering, as well, that RNs will be deployed to provide coverage improvements and a more homogeneous user experience over the cell area, we have systematically deployed RNs at the cell edge at fixed locations. Deployment is done in a way that no coverage gaps are left and overlapping between neighboring RN cells is minimized. The unnecessary holes in RN coverage would deteriorate the relative coverage extension gain from RN deployments, while the overlap between RN cells would lead to inefficient RN deployment.

In the considered two-hop relay based deployment, each UE is either served directly by an eNB or indirectly via an RN. The considered relay deployment along with the links is depicted in Fig. 1. Cell selection for the UEs is based on the strongest downlink received signal power, whereas RNs are connected to the overlaying macrocell. As can be seen in Fig. 1, relay-UEs are mostly the cell edge users and other macro eNB-served UEs (macro-UEs) are mostly in the cell center.

A 20 dB penetration loss is added along with distance dependent path loss in direct and access links, since indoor users are considered. Yet, relays are located outdoors and thus there is no penetration loss in the relay link.

B. UE Scheduling

A resource fair round robin (RR) scheduler allocates the same number of resources to all UEs. That is,

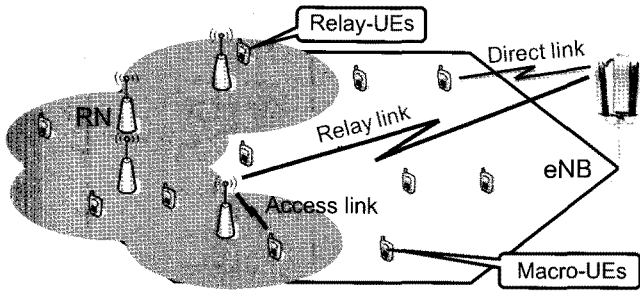$$M_u = \frac{M_{\mathrm{total}}}{N}, \quad u = 1, 2, \cdots, N \tag{5}$$

Fig. 1. One-tier relay deployment shown in a sector. 4 RNs are deployed at the cell-edge.

Fig. 2. FDD LTE-Advanced frame structure considering type 1 RNs. Transmission is abbreviated by Tx.

where N is the number of active UEs in a cell. In our work, we consider modified resource fair RR scheme which takes into account adaptive transmission bandwidth presented in subsection II-D. To be specific, if there are no power-limited UEs for a given UE drop, the scheduling scheme converges to resource fair RR. On the other hand, if there exist some power-limited UEs in the cell, modified resource fair RR first assigns the resources to these users according to their respective $M_{\max,u}$. Afterward, the remaining resource budget will be equally distributed among other users. A formulation of modified resource fairness is presented in [30]. Note that the modified resource fairness converges to the resource fairness as the number of served UEs increases.

C. Resource Sharing

The performance of relay-enhanced networks depends significantly on the resource allocation strategy, i.e., on the balance between different links which compete for resources or which may act as bottlenecks for other consecutive links. For relay-UEs, the experienced end-to-end TP depends on the qualities of both the access and relay links. That is,

$$TP_{\text{end-to-end}} = \min\left(TP_{\text{eNB-RN}}, TP_{\text{RN-UE}}\right) \qquad (6)$$

where end-to-end throughput is obtained as a minimum over throughputs on the relay and access links. In other words, the throughput achieved on the better link will be throttled to accommodate only whatever passes through the bottleneck. As for type 1 RNs, relay and access link transmissions are time-division multiplexed depending on the resource allocation strategy and either of the links may be the bottleneck and can limit the performance. On the other hand, for type 1b RNs, if enough isolation between the access and relay links can be obtained, then both links can be operated simultaneously, i.e., full-duplex operation, thus easing the limitations on the relay link. We note that there will be always some interference between relay and access links if they are operated on the same band. Yet, the amount of self-interference in type 1b relaying depends on the practical issues like antenna arrangements and may largely vary between different deployments. Therefore, we aim to find the maximum performance difference between type 1 and type 1b relays and we ignore the impact of self-interference in case of type 1b relays. Then,

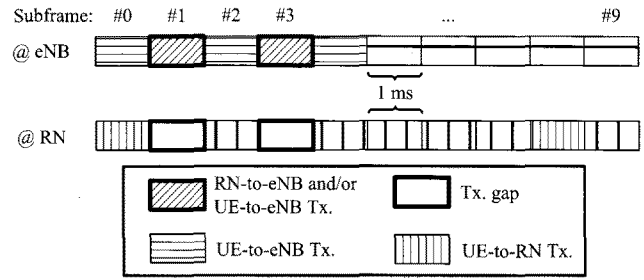$$TP_{\text{end-to-end}} = TP_{\text{RN-UE}}. \qquad (7)$$

This is a rough idealization and actually type 1b relay performance is then comparable with pico base station performance. Since pico base stations and relays in 3GPP admit slightly different radio frequency (RF) configurations, we will use in the following comparisons the term 'type 1b relay' instead of 'pico base station'.

In the following, we present the frame structure and resource allocation rules within the LTE-Advanced framework for type 1 RNs.

C.1 Frame Structure in FDD LTE-Advanced Networks

Given the expected full frequency reuse in LTE-Advanced networks, macro-UEs and relay-UEs are served simultaneously on the same frequency band by eNBs and RNs, respectively. Due to time-division multiplexed feature, while RN is transmitting to its donor eNB on the relay link, it cannot receive transmissions from its relay-UEs on the access link. This is depicted in Fig. 2 where, as exemplified, two backhaul subframes are reserved for relay link transmissions and thus a data transmission gap is experienced on the access link. During the transmission gaps relay-UEs are not scheduled. This subframe structure allows backwards compatibility with LTE Rel. 8. In addition, the set of backhaul subframes is semi-statically assigned, where a maximum of 6 subframes can be configured out of the subframes 1, 2, 3, 6, 7, and 8 [5]. Note that both macro-UEs and RNs can be optionally co-scheduled on such subframes. In this work, unless otherwise stated, we assume, for simplicity, that subframes configured for relay link transmissions are assigned exclusively to RNs at the eNB, i.e., co-scheduling of macro-UEs and RNs is not allowed.

C.2 Resource Allocation in Relay Scenario

For the resource allocation on the relay and access links we propose a combination of relay link scheduling based on the number of relay-UEs and a TP throttling technique achieving max-min fairness on the access link. The scheme is referred to as hop-optimization model [32], [33]. In the hop-optimization model the resource shares of the RNs on the relay link are determined according to the ratio of n_u, the number of UEs attached to an RN u, to the total number of relay-UEs U_{RN}. Thus, the number of resources assigned to an RN is given in terms of the total relay link resources M_{total} as

$$M_u = \frac{n_u}{U_{\text{RN}}} M_{\text{total}}, \quad u = 1, 2, \cdots, N_{\text{RN}} \qquad (8)$$

where N_{RN} is the number of active RNs in the cell. In other words, the resources are allocated to each RN proportional to the number of attached relay-UEs. The available capacity on the relay link is then distributed among relay-UEs utilizing max-min fairness. That is, the relay-UEs with worse access link qualities are to be satisfied first analogously to water filling approach. Consequently, this will increase the end-to-end TP levels at low TP regime at the expense of a relatively lower degradation at high TP regime. Note that the upper bound on the access link capacity of a UE is set by the applied UE scheduling scheme as described in subsection III-B. Moreover, the number of backhaul subframes to be allocated to RNs is chosen such that the overall system performance is optimized.

D. Propagation Scenarios

We consider urban (3GPP case 1) and suburban (3GPP case 3) scenarios with ISDs of 500 m and 1732 m, respectively [5]. Urban scenarios are interference-limited because of small ISD. Yet, small ISD as well implies less power-limited UEs in the macrocell for a given P_0 value. On the contrary, suburban scenarios are coverage-limited because of large ISD. As a direct consequence, the cell-edge UEs in the suburban macrocell can be easily driven to power limitation even with one PRB assignment. This discussion highlights one of the advantages of the relay deployment, which is the decreased radio distance to the access node. As a consequence, using appropriate PC settings the number of power-limited users can be decreased, which is beneficial in terms of user battery life-time.

Both urban and suburban scenarios apply a probabilistic dual-slope channel model on all three links. This channel model defines a line-of-sight (LOS) probability function versus the distance towards the access node. Besides, according to a random probability factor, the node could be in either LOS or non-line-of-sight (NLOS) propagation conditions. The parameters are given in Table 1. Moreover, the total RN coverage areas of one-tier (4 RNs) deployments in the overlaying macrocells are observed as 29.5% and 43.5% for urban and suburban scenarios, respectively.

E. Relay Site Planning

As previously discussed, the end-to-end performance of the relay-UEs depends significantly on the capacity of the relay link. Nevertheless, relay-UEs experience abundance of resources in the RN cell covering relatively a small area, whereas on the relay link, RNs vie for resources at eNB. This renders the relay link a bottleneck. To alleviate such a problem, RN site planning techniques can be utilized. In [5] two models are suggested to simulate the gain due to relay site planning. In this work, we employ the implicit modeling which is to the benefit of the simulation run-time. In particular, an increased LOS probability is considered and a bonus of 5 dB is added on the relay link when experiencing NLOS propagation conditions. Furthermore, if the RN experiences NLOS propagation conditions towards its donor eNB, it is assumed that all other interfering links are in NLOS as well. In addition, the interfering links can be in LOS conditions, only if the RN has LOS link towards its donor eNB. This condition is a direct consequence of relay site planning, where the best relay location is searched such that a better link towards

Table 1. Propagation scenarios.

Distance	R [km]
Path-loss	PL [dB]

Urban scenario-ISD 500 m

eNB-UE link
PL(LOS): $103.4 + 24.2\log_{10}(R)$, PL(NLOS): $131.1 + 42.8\log_{10}(R)$
Prob(LOS) = $\min(0.018 / R, 1)(1 - \exp(-R / 0.063)) + \exp(-R / 0.063)$

RN-UE link
PL(LOS): $103.8 + 20.9\log_{10}(R)$, PL(NLOS): $145.4 + 37.5\log_{10}(R)$
Prob(LOS) = $0.5 - \min(0.5, 5\exp(-0.156/R)) + \min(0.5, 5\exp(-R/ 0.03))$

eNB-RN link
PL(LOS): $100.7 + 23.5\log_{10}(R)$, PL(NLOS): $125.2 + 36.3\log_{10}(R)$
Prob(LOS) = $\min(0.018 / R, 1) (1 - \exp(-R / 0.072)) + \exp(-R / 0.072)$

Suburban scenario-ISD 1732 m

eNB-UE link
PL(LOS): $103.4 + 24.2\log_{10}(R)$, PL(NLOS): $131.1 + 42.8\log_{10}(R)$
Prob (LOS) = $\exp(-(R - 0.01) / 0.2)$

RN-UE link
PL(LOS): $103.8 + 20.9\log_{10}(R)$, PL(NLOS): $145.4 + 37.5\log_{10}(R)$
Prob(LOS) = $0.5 - \min(0.5, 3\exp(-0.3/R)) + \min(0.5, 3\exp(-R / 0.095))$

eNB-RN link
PL(LOS): $100.7 + 23.5\log_{10}(R)$, PL(NLOS): $125.2 + 36.3\log_{10}(R)$
Prob(LOS) = $\exp(-(R - 0.01) / 0.23)$

donor eNB is obtained along with possibly shadowed links towards the interferers [34].

F. Rate Function

The data rate that can be achieved per PRB is calculated from the SINR by using the mapping.

$$TP = S \times \begin{cases} 0, & \text{SINR} < \text{SINR}_{\min} \\ BW\rho_{\max}, & \text{SINR} \geq \text{SINR}_{\max} \\ BWB_{\text{eff}} \log_2\left(1 + A_{\text{eff}}\text{SINR}\right), & \text{otherwise} \end{cases}$$
(9)

where BW is the bandwidth per PRB, $\rho_{\max}$ is the maximum spectral efficiency depending on the highest available MCS for a given $\text{SINR}_{\max}$, and B_{eff} and A_{eff} are the so-called bandwidth and SINR efficiencies [35]. Besides, S is the overhead scaling which accounts for LTE uplink overhead through, e.g., reference signals. The approximation in (9) is obtained from the well-known Shannon link capacity after attenuating and truncating by the aforementioned parameters [36]. Such a mapping is used to model the adaptive MCS applied in the system. The applied bandwidth and SINR efficiencies are given in Table 2. Moreover, we have used $\text{SINR}_{\min} = -7$ dB limit on SINR, i.e., a PRB cannot be correctly utilized for data transmission, if it experiences SINR levels less than -7 dB and then the throughput is set to zero. This limit is introduced due to control channel requirements.

G. Simulation Parameters

The simulated network is represented by a regular hexagonal cellular layout with 19 tri-sectored sites, i.e., 57 cells in total. Simulation parameters are summarized in Table 2.

Table 2. Simulation parameters.

Parameter	Value
System parameters	
Carrier frequency	2 GHz
Bandwidth	10 MHz
Number of PRBs	48 for data + 2 for control channel
PRB bandwidth	180 kHz
Highest MCS	64-QAM, R = 9/10 (ρ_{max} = 5.4 bps/Hz)
Penetration loss	20 dB on eNB-UE and RN-UE links
Bandwidth efficiency	0.88
SINR efficiency	1/1.25
Overhead scaling (S)	0.75
Thermal noise PSD	−174 dBm/Hz
SINR lower bound	−7 dB
eNB parameters	
Transmit power	46 dBm
Elevation gain	14 dBi
Antenna configuration	Tx-2, Rx-2
Noise figure	5 dB
Antenna pattern (horizontal)	$A(\theta) = -\min[12(\theta/\theta_{3\text{ dB}})^2, A_m]$ $\theta_{3\text{ dB}} = 70°$ and $A_m = 25$ dB
UE parameters	
Maximum transmit power	23 dBm
Antenna configuration	Tx-1, Rx-2
Maximum antenna gain	0 dBi
Noise figure	9 dB
RN parameters	
Relay site planning	Considered via higher probability of LOS and 5 dB bonus on NLOS
Transmit power	30 dBm
Antenna configuration	Tx-2, Rx-2
RN-eNB elevation gain (directional antenna)	7 dBi
RN-UE elevation gain	5 dBi
Relay link antenna pattern (horizontal)	$A(\theta) = -\min[12(\theta/\theta_{3\text{ dB}})^2, A_m]$ $\theta_{3\text{ dB}} = 70°$ and $A_m = 20$ dB
Access link antenna pattern	Omni-directional
Noise figure	5 dB
Shadowing	
Shadow fading	Log-normal
Standard deviation	8 dB on the direct link 10 dB on the access link 6 dB on the relay link
De-correlation distance	50 m
Correlation factor	0.5 between sites 1.0 between sectors

Indoor users are assumed, where 25 uniformly distributed UEs are dropped per sector and the full buffer traffic model is applied. In total, 200 user drops (or snap-shots) are simulated using a Matlab based system level semi-static simulator, where results are collected from the inner most sector only, to ensure proper modeling of interference (two tiers of tri-sector sites). The number of drops is selected to be large enough such that the difference between repeated tests is ignorable.

A frequency reuse factor of one (full reuse scheme) is considered among the RNs and macrocells in the network. All available resources in a cell are assumed to be used and hence, a rather pessimistic interference modeling is considered on the access link, i.e., relay-UEs are assumed to be always transmitting on all PRBs.

Two antenna sets are considered for RNs. Directional antennas are assumed at the RNs for backhaul transmission, while omni-directional antennas are assumed for the access link transmission. Log-normal shadow fading is as well modeled and applied for NLOS propagation conditions only, while fast fading is not simulated.

IV. PERFORMANCE EVALUATION AND ANALYSIS

Following the discussion in subsection II-D, adaptive transmission bandwidth is considered only for suburban scenarios. Besides, for type 1 RNs, the number of backhaul subframes is, respectively, set to 2 and 4 for urban and suburban scenarios [32]. These settings are found to optimize the overall system performance along with more homogeneous user experience over the whole cell area.

The rest of this section is organized as follows. First, geometry analyses are provided for type 1 RNs to highlight the impact of directional antenna installation at RNs and relay site planning on the relay link quality. Second, the PC optimization strategies are presented. The performances of type 1 and type 1b RNs are analyzed and compared in urban and suburban scenarios. The analyses are supported by comprehensive system level simulations.

A. Geometry Analysis for Type 1 RNs

The relay link quality has great influence on the overall performance of type 1 RNs. Therefore, we explore the impact of directional antennas and relay site planning on the relay link geometry. Accordingly, four settings are defined.

- Setting A: No directional antennas at RNs and no relay site planning. This is the reference setting.
- Setting B: Only directional antennas at RNs.
- Setting C: Only relay site planning.
- Setting D: Both directional antennas at RNs and relay site planning.

The corresponding geometry CDFs for urban and suburban scenarios are shown in Fig. 3. It can be observed that for all configurations, the relay link has better geometry in urban scenarios due to smaller ISD. Very low geometry values are experienced when there is neither directional antenna installation nor relay site planning. This degradation is significant for suburban case for low geometry regime. Thus, relay site planning is necessary especially when some RNs are needed to be served by specific donor eNBs. Significant geometry improvement is seen when
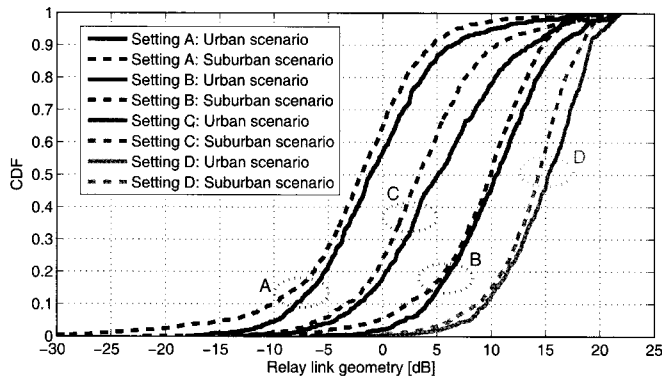
Fig. 3.   Relay link geometry for urban and suburban scenarios under different configurations.

Fig. 4. Cell capacity vs. 5%-ile user TP for different values of α in eNB-only deployment. The hull curve depicts the trade-off between cell coverage and cell capacity.

Table 3. Parameter configurations for eNB-only deployment.

	Cell coverage-oriented	Cell capacity-oriented
P_0 [dBm] & α	-101 & 1.0 (FCPC)	-55 & 0.6 (FPC)
avgIoT [dB]	10.1	16.8
Cell capacity [kbps]	9404	12220
5%-ile user TP [kbps]	4200	3020

directional antennas are installed, which results in lower interference levels. As expected, the best performance is obtained when both directional antennas are installed and relay site planning is applied. Therefore, setting D is configured as default in the following sections.

B. Urban Scenarios (ISD 500 m)

We first develop a PC optimization strategy which is common for both type 1 and type 1b RNs. Then, the impact of relaying overhead on the performance of type 1 RNs will be discussed in detail. We suggest different parameter configurations aiming at optimizing different system performance metrics.

In urban scenarios due to smaller ISD, the inter-cell interference becomes decisive rather than the wanted signal level. That is, thanks to uplink PC the path loss, including shadowing, can be effectively compensated such that target received SNR can be reached for all users. Thus, a smaller ISD also implies a more homogeneous user experience in the coverage area depending on the PC strategy.

B.1 Common PC Optimization Strategy

The common PC optimization strategy for type 1 and type 1b RNs comprises four steps.
1 Optimization in eNB-only scenario.
2 Applying optimized eNB-only parameter settings both at eNBs and RNs in relay scenario.
3 Relay scenario specific optimization at RNs.
4 Relay scenario specific optimization at eNBs.

B.1.a Optimization in eNB-Only Scenario (Step 1)

A parameter sweep over P_0 set is applied for four different values of. Obtained cell capacity and 5%-ile user TP values are plotted in Fig. 4. For a given value, each operating point corresponds to a specific P_0 value and average interference over thermal (avgIoT) level of the system. avgIoT is determined by taking the harmonic mean of IoT as follows.

$$\text{avgIoT} = \frac{1}{E_{f,t}\{\frac{1}{\text{IoT}}\}} \tag{10}$$

where $E_{f,t}\{\}$ is the expectation over frequency and time. Average IoT is a good measure for the operating point of the system,
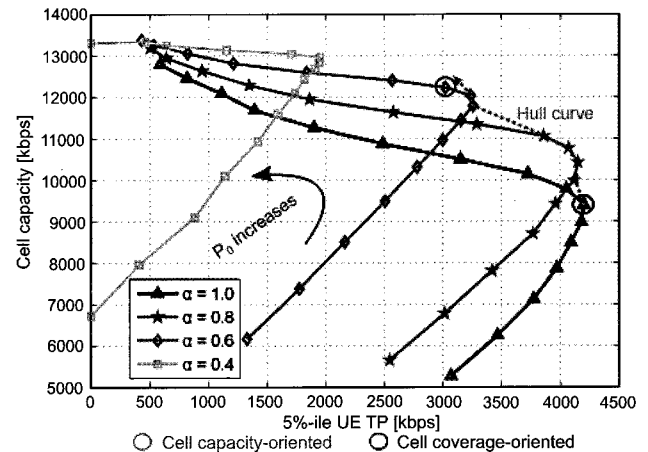
since it is related to the average SINR of the system as

$$E_{f,t}\{\text{SINR}\} = \frac{\frac{P_w}{P_N}}{\text{avgIoT}} \tag{11}$$

where P_w is the power of the wanted signal and P_N is the thermal noise power per PRB. Recall that interference over thermal (IoT) indicates the amount of inter-cell interference in uplink and thus high IoT values are not desirable because of the limitations in the receiver dynamic range. In Fig. 4, for a given curve moving from lower left corner to upper left corner, P_0 value increases, which also implies a higher avgIoT. Fig. 4 reveals the optimum parameter settings such that FCPC ($\alpha = 1.0$) is suggested when cell coverage is prioritized. Following the shown hull curve, the path loss compensation factor of 0.6 provides the optimum performance when cell capacity is decisive. Note that, the hull curve indicates the optimum performance points where at the final point the percentage-wise increase in cell capacity is higher than the percentage-wise decrease in 5%-ile user TP. The selected parameter settings are presented in Table 3 together with 5%-ile user TP and cell capacity.

The comparison of the settings shows that the capacity-oriented scheme utilizing FPC results in 30% capacity gain over the coverage-oriented scheme utilizing FCPC at the cost of a 5%-ile user TP loss of 28%.

B.1.b Common Parameter Settings at eNB and RN (Step 2)

The parameter settings optimized for the eNB-only deployment are applied both at RNs and eNBs in the relay scenario. As a reference for the performance comparisons, the eNB-only deployment with cell capacity-oriented setting is considered. Note
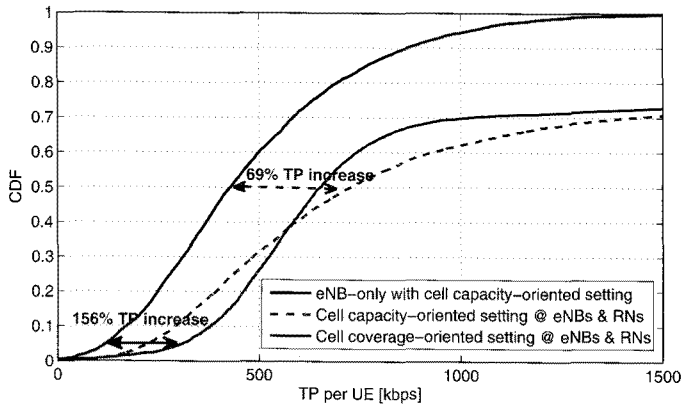
Fig. 5. CDF of TP per UE for common settings at eNBs and RNs. These simulation results show the explicit performance of type 1b RNs. The two lowermost CDF curves go to one at very high TP levels.

Fig. 6. Mean IoT at eNB vs. $P_0^{\rm RN}$ for different $P_{\rm max}^{\rm RN}$ values. The simulation results are given for FPC and FCPC settings. eNB-only settings are denoted by ellipses.

that for the following simulation results the relaying overhead is not considered, i.e., the achieved TP levels at direct and access links are taken into account. Thus, these results show the explicit performance of type 1b RNs only. The relaying overhead of type 1 RNs will be considered in the following sections.

It is worth emphasizing that the users which experience low SINR at the cell edge of the eNB-only deployment are connected to RNs after the relay deployment is introduced. As it can be observed in Fig. 5, the relay deployment outperforms the eNB-only deployment both in terms of cell coverage and cell capacity. The users served by RNs experience very high TP compared to the ones served by eNBs due to the fact that RNs mostly serve a small number of users in their coverage areas. This in turn leads to very large bandwidth allocation for each user and high uplink TP at the RNs.

The use of the parameter settings of the eNB-only deployment in the one-tier relay scenario leads to a state where the cell coverage-oriented setting at eNBs and RNs provides higher TP for the users up to 38%-ile level of the TP curve, whereas cell capacity-oriented setting at eNBs and RNs provides better performance for the remaining users. Moreover, the cell coverage-oriented setting at eNBs and RNs shows 156% TP gain over eNB-only deployment at 5%-ile TP CDF level. The cell capacity-oriented setting at eNBs and RNs boosts the performance by 69% relative to eNB-only deployment at 50%-ile TP CDF level.

It is as well observed that the users in RN cells experience very high TPs while causing interference to the users connected to eNBs. As we focus on achieving a homogeneous user experience over the whole cell area, being a requirement for LTE-Advanced, the power control parameter configuration after the deployment of RNs in the system can be adjusted to further improve the performance macro-UEs.

B.1.c Relay Scenario Specific Optimization at RNs (Step 3)

The total inter-cell interference at eNB determines the performance of the macro-UEs. After RNs are deployed, the total interference at eNB increases due to the transmission of relay-UEs. In this concept, the interference caused by relay-
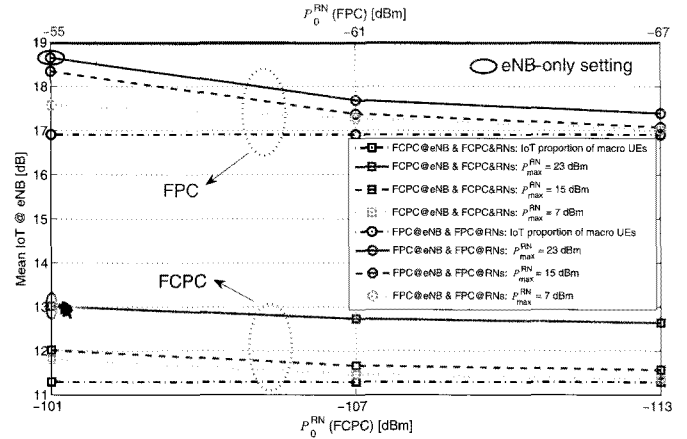
UEs and macro-UEs can be analyzed separately. Assuming incoherent addition of interfering signals, the instantaneous IoT per PRB in linear domain can be written as

$$\mathrm{IoT} = \frac{I + P_N}{P_N} = \frac{I_{\rm macro\text{-}UEs} + I_{\rm relay\text{-}UEs} + P_N}{P_N} \qquad (12)$$

where $I_{\rm macro\text{-}UEs}$ and $I_{\rm relay\text{-}UEs}$ are two random variables which refer to interference caused by macro-UEs and relay-UEs, respectively. Equation (12) can be rewritten as

$$\mathrm{IoT} = \frac{I_{\rm macro\text{-}UEs} + P_N}{P_N} + \frac{I_{\rm relay\text{-}UEs} + P_N}{P_N} - 1. \qquad (13)$$

Applying the expectation operator to the both sides of (13) the mean IoT at eNB and the interference proportions of the macro-UEs and relay-UEs can be formulated as

$$E_{f,t}\{\mathrm{IoT}\} = E_{f,t}\{\mathrm{IoT}_{\rm macro\text{-}UEs}\} + E_{f,t}\{\mathrm{IoT}_{\rm relay\text{-}UEs}\} - 1 \qquad (14)$$

where $E_{f,t}\{\mathrm{IoT}_{\rm macro\text{-}UEs}\}$ and $E_{f,t}\{\mathrm{IoT}_{\rm relay\text{-}UEs}\}$ are the macro-UE and relay-UE IoT proportions, respectively. In order to increase the performance of the macro-UEs, the IoT proportion of the relay-UEs can be decreased. This analysis is presented in Fig. 6 for FPC and FCPC settings, where decreasing P_0 and $P_{\rm max}$ in RN cells decreases mean IoT at eNB as a result of decreased IoT proportion of the relay-UEs.

For FPC, when $P_0 < -61$ dBm, the decrease of the interference of relay-UEs does not translate into significant decrease in the mean interference at eNB. Moreover, it can be observed that the mean interference at eNB converges to the interference of the macro-UEs as this interference becomes dominant. Since for $P_0 = -61$ dBm different $P_{\rm max}$ values show similar performance, the receiver dynamic range of the RN becomes decisive. The receiver dynamic ranges for $P_{\rm max} = 23$ dBm, 15 dBm, and 7 dBm are 10.1 dB, 10.2 dB, and 11.2 dB, respectively. Additionally, rendering the upper limit of the receiver dynamic range, no power control scheme with $P_{\rm max} = 7$ dBm has 14 dB of receiver dynamic range. It can be seen that no power control and FPC with $P_{\rm max} = 7$ dBm are subject to higher receiver dynamic ranges, which is not desired. Among $P_{\rm max} = 23$ dBm and

P_{max} = 15 dBm, lower P_{max} is advantageous from a UE battery lifetime point of view. We note that, more reduction in P_0 and P_{max} of RNs will yield drastic performance degradation for relay-UEs which cannot justify the slight performance increase for macro-UEs.

For FCPC, it can be observed that for P_0 = −101 dBm reducing P_{max} in RN cells from 23 dBm to 15 dBm already results in the possible mean IoT reduction at eNB. Thus, further reduction in P_0 and P_{max} of RNs is not necessary. This behavior is a direct consequence of FCPC, where P_{max} reduction mainly decreases the power levels of cell-edge users who are transmitting with high powers due to high path-loss. Besides, the receiver dynamic range at RN becomes 9.2 dB.

It is worth mentioning that, from system perspective, the simplest approach is to fix the uplink transmit power and not to apply power control since this scheme allows a simple implementation and operation procedure. However, the high receiver dynamic range should then be handled by the scheduler, which in turn increases the scheduler complexity.

B.1.d Relay Scenario Specific Optimization at eNB (Step 4)

The performance of macro-UEs can be further improved by means of accepting higher IoT from the macro-UEs by increasing the P_0 value optimized in the eNB-only deployment.

A parameter sweep over P_0 set is applied for FPC and FCPC at eNBs while fixing the power control scheme at RNs according to the optimization step 3. Since the design goal is to maximize the macro-UE performance, the results of 50%-ile user TP vs. 5%-ile user TP are shown in Fig. 7. In addition, the dashed curves depict the case where the PC setting obtained in step 2 is configured for the RNs. It can be observed that significant performance improvement is obtained for FPC over the P_0 set of interest, when step 3 parameters are applied. For FCPC, such performance improvement is moderate.

When considering the solid curves, two configurations can be suggested. Following the hull curve I, 5%-ile user TP can be further increased reaching the cell coverage-oriented configuration. On the other hand, 50%-ile user TP can be further increased following the hull curve II at the cost of a decrease in 5%-ile user TP.

The optimized parameter configurations and achieved TP gains with respect to eNB-only deployment with FPC are presented in Table 4. It is observed that by means of further optimization significant TP gains are obtained both at 50%-ile and 5%-ile user TP levels. These results reflect the explicit performance of type 1b RNs and the achievable TP levels for type 1 RNs. In the following section, we will discuss the impact of the relaying overhead on the overall performance of type 1 RNs.

B.2 Relaying Overhead for Type 1 RNs

The required isolation between relay and access links for type 1b RNs may not be desired for specific scenarios due to increased deployment costs. Hence, it is important to analyze the performance improvement of type 1 RNs under relaying overhead. We recall that the hop-optimization model presented in subsection III-C is applied for the multi-hop link (UE-RN-eNB).

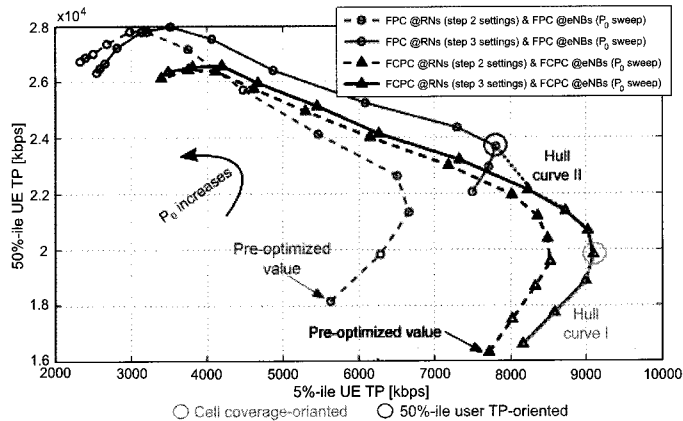First, optimum PC configuration for the relay link is investi-

Fig. 7. 50%-ile user TP vs. 5%-ile user TP for FPC and FCPC.

Table 4. Optimized parameter configurations after step 4.

Parameters		50%-ile user TP-oriented		Cell coverage -oriented	
		eNBs	RNs	eNBs	RNs
P_0 [dBm]		-51	-61	-95	-101
α		0.6	0.6	1.0	1.0
P_{max} [dBm]		23	15	23	15
TP gain w.r.t. eNB-only with FPC	@50%-ile	121%		85%	
	@5%-ile	159%		201%	

gated. Relatively better link towards donor eNB and the requirement for high capacity suggest the cell capacity-oriented setting as an appropriate starting point. Therefore, the cell capacity-setting found in step 1 is used as the PC setting for the relay link. A P_0 sweep around this setting is applied and the 50%-ile TP gains relative to eNB-only deployment with FPC are determined at each P_0 value. For the macro-UEs and relay-UEs the settings found in step 4 are configured. Second, in order to analyze the effect of co-scheduling of macro-UEs and RNs during a backhaul subframe, the values of eNB receiver dynamic range at each P_0 setting are calculated as well. The eNB receiver dynamic range is calculated by combining the statistics of macro-UEs together with the statistics of RNs. Thus, the calculated values form an upper bound for the receiver dynamic range. We note that the co-scheduling of macro-UEs and RNs might be necessary for the specific cases, e.g., when RNs serve users with low quality of service requirements and there are macro-UEs with higher quality of service requirements.

The simulation results are presented in Fig. 8 for 50%-ile user TP-oriented and cell coverage-oriented settings applied at UEs along with cell capacity-oriented setting applied at relay link. A receiver dynamic range of 20 dB is taken as the upper limit. In Fig. 8(a), it is observed that the TP gain saturates as of $P_0^{\text{Relaylink}}$ = −55 dBm and the receiver dynamic range is lower than the upper limit. Similarly, in Fig. 8(b), it is seen that the TP gain almost saturates as of $P_0^{\text{Relaylink}}$ = −53 dBm and this setting yields a receiver dynamic range that is just below the upper limit. Consequently, these values are configured for the relay
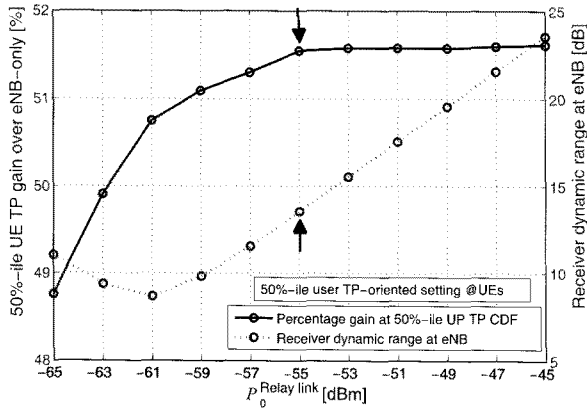
(a)
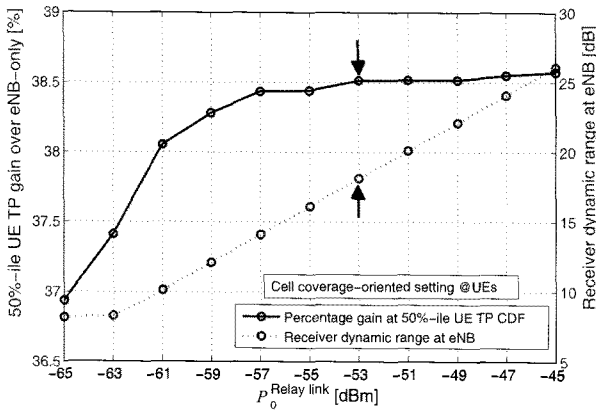
(b)

Fig. 8.   50%-ile user TP gain w.r.t. eNB-only deployment and eNB receiver dynamic range vs. $P_0^{\text{Relaylink}}$ (with FPC): (a) 50%-ile user TP-oriented setting and (b) cell coverage-oriented settings applied at UEs.

link.

The corresponding UE TP CDFs are presented in Fig. 9 for type 1 and type 1b RNs. Moreover, the dotted curves show the case where the relay link is ideal. The performance degradation relative to type 1b is then due to time-division multiplexed feature of the relay link where UEs are not scheduled. Thus, these curves provide the upper limits that can be achieved by type 1 RNs. It is seen that type 1 RNs with both settings can achieve these upper limits up to 7% thanks to applied hop-optimization model. We recall that the hop-optimization model satisfies the low TP regime first and achieves max-min fairness for the relay-UEs. In addition, relative to eNB-only deployment, type 1 RNs with cell coverage-oriented setting applied at UEs achieve 140% and 39% performance enhancement at 5%-ile and 50%-ile user TP CDF levels, respectively. Furthermore, 50%-ile user TP oriented setting applied at UEs achieves 119% and 52% gains at 5%-ile and 50%-ile user TP CDF levels, respectively. Thus, the latter boosts the performance for higher TP regime enabling a good trade-off. Note that the performance gains for type 1b RNs were tabulated in Table 4. Both RN types show significant performance enhancement relative to eNB-only deployment. Although, relaying overhead results in performance degradation,
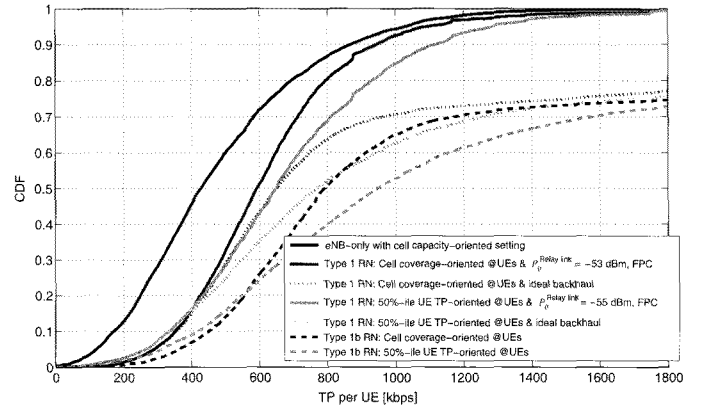

Fig. 9.   UE TP CDFs for type 1 and type 1b RNs. The optimized PC settings are applied.

type 1 RNs promise a cost-efficient deployment.

C. Suburban Scenarios (ISD 1732 m)

In contrary to urban scenarios due to larger ISD, the impact of inter-cell interference decreases drastically in suburban scenarios. On the other hand, path-loss of cell edge UEs may not be compensated for and they can be easily driven to power limitation even if one PRB is assigned. The result is inhomogeneous user experience over the cell area where cell center UEs experience high TP levels because of reduced inter-cell interference and cell edge UEs suffer from high path loss. Thus, suburban scenarios are coverage-limited. In addition, adaptive transmission bandwidth, presented in subsection II-D, is an essential feature for suburban scenarios in order to prevent outage of cell edge UEs. That is, due to lower SINR limit, the resource assignment should be done carefully. Assigning more resources to power limited UEs will result in reduced transmit power level per PRB and hence too less SINR.

In this section, we develop a PC optimization strategy for suburban scenarios. The optimization strategy takes into account the inhomogeneity of the user experience via jointly optimizing several performance metrics. First, the common PC optimization strategy is presented for type 1 and type 1b RNs. Then, the impact of relaying overhead on the performance of type 1 RNs will be discussed in detail.

C.1 Common PC Optimization Strategy

As the inter-cell interference is less pronounced in suburban scenarios, the approach based on interference proportions used for urban scenarios is not appropriate for suburban scenarios. Instead, the system performance metrics are jointly optimized to guarantee an enhancement in overall system performance. The common PC optimization strategy for type 1 and type 1b RNs comprises three steps.

1 Joint parameter optimization in eNB-only scenario.
2 Applying optimized eNB-only parameter setting both at eNBs and RNs in relay scenario.
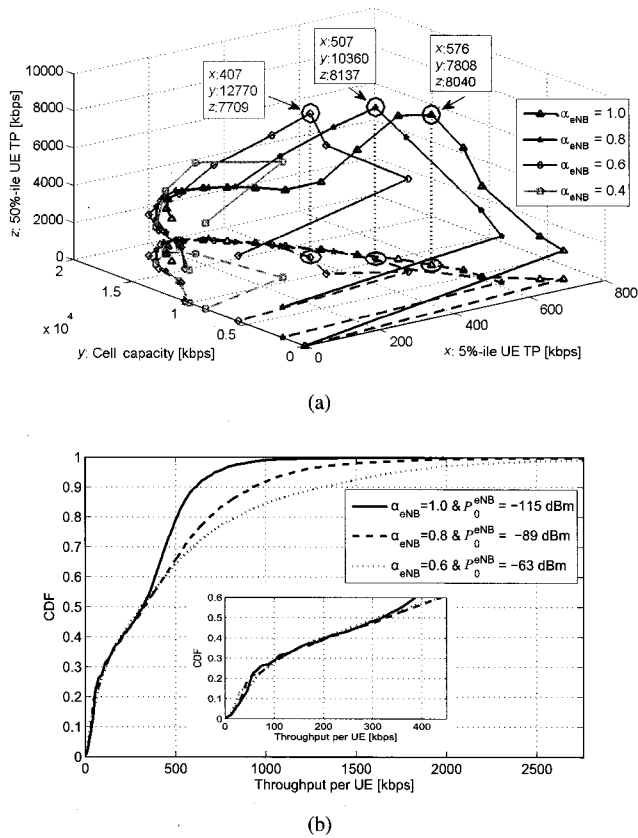3 Joint parameter optimization in relay scenario.

(a)

(b)

Fig. 10. (a) 5%-ile user TP vs. cell capacity vs. 50%-ile user TP for different values of α in eNB-only deployment. Three candidate settings can be observed with tagged TP levels and (b) UE TP CDFs for these settings.
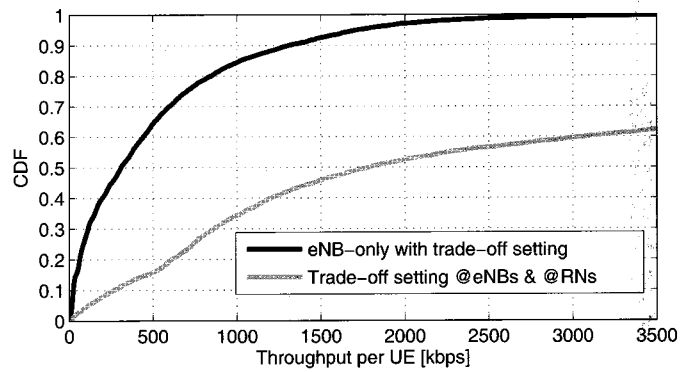

Fig. 11. CDF of TP per UE for common settings at eNBs and RNs. These simulation results show the explicit performance of type 1b RNs. The lowermost CDF curve goes to one at very high TP level.

C.1.a Joint Optimization in eNB-Only Scenario (Step 1)

A parameter sweep over P_0 set is applied for four different values of. Obtained cell capacity, 50%-ile user TP and 5%-ile UE TP values are plotted in Fig. 10(a). Note that such 3-metric (3-M) optimization is critical to assure an optimum performance enhancement. The projection onto the $x - y$ plane reveals the trade-off between 5%-ile UE TP and cell capacity. Furthermore, taking 50%-ile UE TP into account, three candidate settings with tagged TP levels can be obtained as depicted in the figure. Besides, UE TP CDFs of these candidate settings are presented in Fig. 10(b). According to Fig. 10(b), it can be observed that $\alpha = 0.6$ with $P_0 = -63$ dBm enables a good trade-off between these three performance metrics. This setting is referred to as the trade-off setting in the following. In addition, with the trade-off setting the eNB receiver dynamic range becomes 10.9 dB.

C.1.b Common Parameter Settings at eNB and RN (Step 2)

The trade-off setting, optimized for the eNB-only deployment, is applied both at RNs and eNBs in the relay scenario. As a reference for the performance comparisons, the eNB-only deployment with the trade-off setting is considered.

The UE TP CDFs are shown in Fig. 11. As expected, eNB-only deployment has very poor 5%-ile UE TP performance (16 kbps). On the contrary, very high TP levels are observed,

as well. The relay deployment significantly outperforms the eNB-only deployment. Namely, relative to eNB-only deployment, 589% and 479% TP gains are observed at 5%-ile and 50%-ile TP CDF levels, respectively. As a next step, a joint power control parameter optimization is done in the relay scenario to search for possible enhancements.

Note that for these simulation results, the relaying overhead is not considered, i.e., the achieved TP levels at direct and access links are taken into account. Thus, these results show the explicit performance of type 1b RNs only. The relaying overhead of type 1 RNs will be considered in the following sections.

C.1.c Joint Optimization in Relay Scenario (Step 3)

A parameter sweep over P_0 set around trade-off setting is applied for macro-UEs and this procedure is repeated for different fixed PC settings at RN cells. P_0 and $P_{\max}$ values for relay-UEs are selected from the sets of $[-57, -63, -69]$ dBm and $[23, 15, 7]$ dBm, respectively. The corresponding 5%-ile and 50%-ile TP levels are determined. It is observed that for $P_{\max}^{\mathrm{RN}} = 7$ dBm the performance of relay-UEs degrades drastically resulting in overall performance degradation. On the other hand, for $P_{\max}^{\mathrm{RN}} = 23$ dBm and $P_{\max}^{\mathrm{RN}} = 15$ dBm similar performances are observed for $P_0^{\mathrm{RN}} \in [-63, -69]$ dBm. Besides, for $P_0^{\mathrm{RN}} = -57$ dBm, $P_{\max}^{\mathrm{RN}} = 15$ dBm outperforms $P_{\max}^{\mathrm{RN}} = 23$ dBm. In addition, a lower $P_{\max}$ is desirable for a longer user battery life-time. Consequently, for the sake of clearness, the simulation results for $P_{\max}^{\mathrm{RN}} = 15$ dBm only are shown in Fig. 12(a). Three settings can be noticed, which can enable a trade-off. These settings are marked in the figure and the corresponding UE TP CDFs are plotted in Fig. 12(b). Moving from setting 0 to setting 1 (decreasing P_0^{RN} by 6 dB) a slight performance improvement can be observed up to 50%-ile CDF level corresponding to macro-UE TP performance, whereas relay-UE performance decreases drastically. Furthermore, moving from setting 0 to setting 2 (increasing P_0^{eNB} by 2 dB), an improvement can be observed as of 20%-ile at the cost of a performance degradation at low TP regime. Thus, it can be seen that the trade-off setting applied at eNBs and RNs can still provide a good compromise. Recall that, different to the trade-off setting $P_{\max}^{\mathrm{RN}} = 15$ dBm is selected for user battery life-time considera-
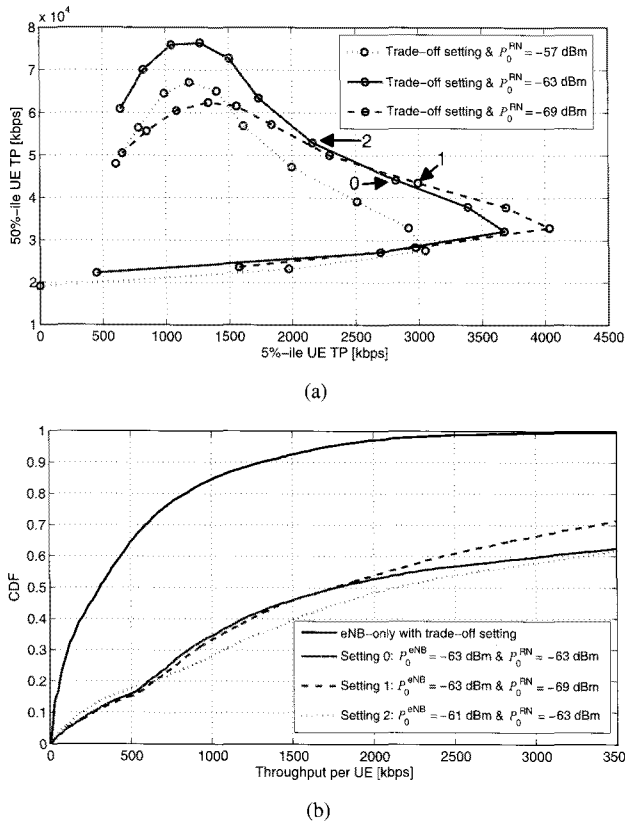
(a)

(b)

Fig. 12. (a) 5%-ile user TP vs. 50%-ile user TP for different values P_0^{RN} in relay deployment. Three settings can be noticed and (b) UE TP CDFs for these settings.
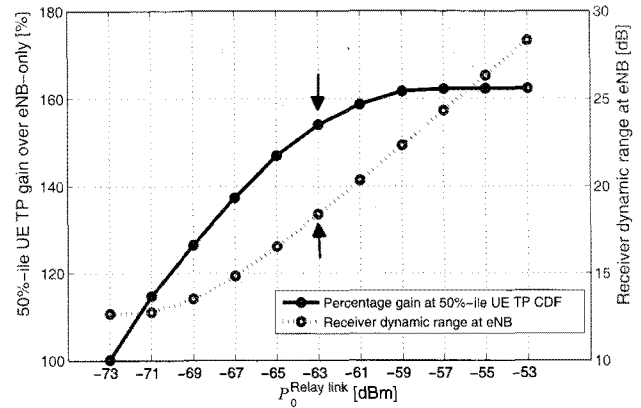

Fig. 13. 50%-ile user TP gain w.r.t. eNB-only deployment and eNB receiver dynamic range vs. $P_0^{Relaylink}$ (with trade-off setting).
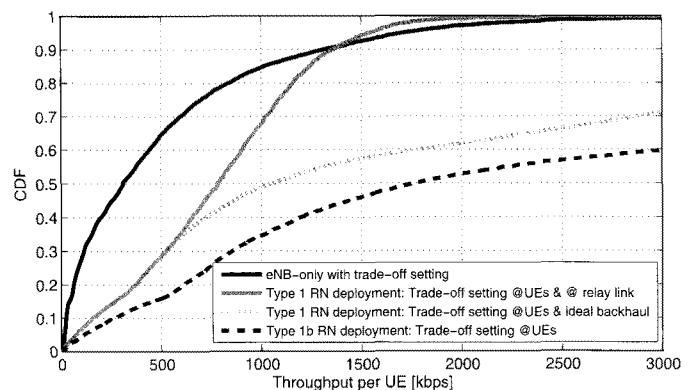

Fig. 14. UE TP CDFs for type 1 and type 1b RNs. The optimized PC setting is applied.

tion.

C.2 Relaying Overhead for Type 1 RNs

In this section, we analyze the impact of the relaying overhead on the performance of type 1 RNs in suburban scenarios. The approach is similar to the one applied in urban scenarios. We recall that the hop-optimization model presented in subsection III-C is applied for the multi-hop link (UE-RN-eNB). The number of backhaul subframes is set to 4 in accordance with the increased coverage area of the RNs in suburban scenarios.

The trade-off setting found in step 1 is used as the PC setting for the relay link. A P_0 sweep around this setting is applied and the 50%-ile TP gains relative to eNB-only deployment are determined at each P_0 value. For the macro-UEs and relay-UEs the setting found in step 3 is configured. Second, in order to analyze the effect of co-scheduling of macro-UEs and RNs during a backhaul subframe, the values of eNB receiver dynamic range at each P_0 setting are calculated as well. The eNB receiver dynamic range is calculated by combining the statistics of macro-UEs together with the statistics of RNs. Thus, the calculated values form an upper bound for the receiver dynamic range.

The simulation results are presented in Fig. 13. Recall that a receiver dynamic range of 20 dB is taken as the upper limit. In Fig. 13, it is observed that despite the upward trend in 50%-ile UE TP gain, for $P_0^{Relaylink} > -63$ dBm the receiver dynamic range becomes higher than the upper limit. Consequently, $P_0^{Relaylink} = -63$ dBm is configured for the relay link.

The corresponding UE TP CDFs are presented in Fig. 14 for type 1 and type 1b RNs. Moreover, the dotted curve shows the case when relay link is ideal. The performance degradation relative to type 1b is then due to the time-division multiplex feature of the relay link where UEs are not scheduled. Thus, this curve provides the upper limit that can be achieved by type 1 RNs. It is seen that type 1 RNs can achieve this upper limit up to 33% thanks to applied hop-optimization model. In addition, relative to eNB-only deployment, type 1 RNs achieve 344% and 154% performance enhancement at 5%-ile and 50%-ile user TP CDF levels, respectively. Note that the performance gains for type 1b RNs were presented in subsection IV-C-1b. Relative to eNB-only deployment, significant performance enhancement can be achieved by both RN types. Despite the performance degradation due to relaying overhead, type 1 RNs promise a cost-efficient deployment also in suburban scenarios.

V. CONCLUSION

An evaluation of the relay based heterogeneous deployment within the LTE-Advanced uplink framework is carried out by applying the standardized LTE Release 8 power control scheme both at eNBs and relay nodes. Different power control optimization strategies are proposed for 3GPP urban (ISD 500 m) and

Table 5. Most important/frequently used abbreviations.

3GPP	Third generation partnership project
eNB	Evolved node B (LTE base station)
FCPC	Full compensation power control
FPC	Fractional power control
IoT	Interference over thermal (noise)
ISD	Inter-site distance
PC	Power control
PDCCH	Physical downlink control channel
PRB	Physical resource block
PUCCH	Physical uplink control channel
PUSCH	Physical uplink shared channel
RN	Relay node
TP	Throughput
TTI	Transmission time interval
UE	User equipment

suburban (ISD 1732 m) scenarios. A comparison between type 1 and type 1b relay nodes is as well presented to study the effect of the relaying overhead on the system performance in inband relay deployments. Besides, the power control is found to be crucial not only to mitigate inter-cell interference but also to assure a proper receiver dynamic range.

First, it has been shown that via proper power control optimization the relay deployments significantly enhance the system performance compared to conventional homogeneous deployments in both urban and suburban scenarios. Moreover, it is observed that poor cell edge performance of homogeneous deployments in suburban scenarios can be effectively coped with by relay deployments. Second, we have seen that especially in high throughput regime, type 1 relays clearly lag behind type 1b relays in throughput performance due to relaying overhead. However, type 1 RNs promise a cost-efficient deployment while type 1b RNs require a high isolation between relay and access links.

After applying the proposed power control optimization strategies, in urban scenarios, type 1 and type 1b RNs achieve, respectively, 140% and 201% gains relative to homogeneous deployment at the 5%-ile user throughput CDF level. Moreover, in suburban scenarios, type 1 and type 1b RNs provide, respectively, 344% and 589% gains relative to homogeneous deployment at the 5%-ile user throughput CDF level.

APPENDIX

The most important/frequently used abbreviations are given in Table 5.

REFERENCES

[1]   Circular Letter 5/LCCE/2. (2008, Mar). Invitations for submission of proposals for candidate radio interface technologies for the terrestrial components of the radio interfaces for IMT-Advanced and invitation to participating in their subsequent evaluation. [Online]. Available: http://www.itu.int

[2]   3GPP RP-090939. 3GPP submission package for IMT-Advanced. [Online]. Available: http://www.3gpp.org

[3]   3GPP TR 36.913. (2009, Dec). Requirements for further advancements for evolved universal terrestrial radio access (E-UTRA). [Online]. Available: http://www.3gpp.org

[4]   A. Ghosh, R. Ratasuk, B. Mondal, N. Mangalvedhe, and T. Thomas, "LTE-advanced: Next-generation wireless broadband technology," IEEE Wireless Commun., vol. 17, no. 3, pp. 10–22, June 2010.

[5]   3GPP TR 36.814. (2010, Mar). Further advancements for E-UTRA: Physical layer aspects (Release 9). [Online]. Available: http://www.3gpp.org

[6]   E. Lang, S. Redana, and B. Raaf, "Business impact of relay deployment for coverage extension in 3GPP LTE-Advanced," in Proc. IEEE ICC, Dresden, Germany, June 2009.

[7]   K. Doppler, S. Redana, M. Wódczak, P. Rost, and R. Wichman, "Dynamic resource assignment and cooperative relaying in cellular networks: Concept and performance assessment," EURASIP J. Wireless Commun. Netw., vol. 2009, Jan. 2009.

[8]   A. So and B. Liang, "Effect of relaying on capacity improvement in wireless local area networks," in Proc. IEEE WCNC, vol. 3, New Orleans, USA, Mar. 2005, pp. 1539–1544.

[9]   A. Bou Saleh, S. Redana, J. Hämäläinen, and B. Raaf, "On the coverage extension and capacity enhancement of inband relay deployments in LTE-advanced networks," J. Electr. Comput. Eng., vol. 2010, 2010.

[10] A. Bou Saleh, S. Redana, J. Hämäläinen, and B. Raaf, "Comparison of relay and pico eNB deployments in LTE-advanced," in Proc. IEEE VTC, Anchorage, USA, Sept. 2009.

[11] R. Schoenen, W. Zirwas, and B. H. Walke, "Capacity and coverage analysis of a 3GPP-LTE multihop deployment scenario," in Proc. IEEE ICC, Beijing, China, May 2008.

[12] R. Schoenen, R. Halfmann, and B. H. Walke, "An FDD multihop cellular network for 3GPP-LTE," in Proc. IEEE VTC, Marina Bay, Singapore, May 2008, pp. 1990–1994.

[13] B. E. Priyanto, T. B. Sorensen, and O. K. Jensen, "In-band interference effects on UTRA LTE uplink resource block allocation," in Proc. IEEE VTC, May 2008, pp. 1846–1850.

[14] G. J. Foschini and Z. Miljanic, "A simple distributed autonomous power control algorithm and its convergence," IEEE Trans. Veh. Technol., vol. 42, no. 4, Nov. 1993.

[15] R. D. Yates, "A framework for uplink power control in cellular radio systems", IEEE J. Sel. Areas Commun., vol. 13, no. 7, Sept. 1995.

[16] N. Jindal, S. Weber, and J. G. Andrews, "Fractional power control for decentralized networks," IEEE Trans. Wireless Commun., vol. 7, no. 12, Dec. 2008.

[17] M. Coupechoux and J. M. Kelif, "How to set the fractional power control compensation factor in LTE?," in Proc. IEEE Sarnoff Symp., 2011.

[18] C. U. Castellanos, D. L. Villa, C. Rosa, K. I. Pedersen, F. D. Calabrese, P.-H. Michaelsen, and J. Michel, "Performance of uplink fractional power control in UTRAN LTE," in Proc. IEEE VTC, Singapore, May 2008, pp. 2517–2521.

[19] A. Simonsson and A. Furuskar, "Uplink power control in LTE–overview and performance," in Proc. IEEE VTC, Canada, Sept. 2008.

[20] C. U. Castellanos, F. D. Calabrese, K. I. Pedersen, and C. Rosa, "Uplink interference control in UTRAN LTE based on the overload indicator," in Proc. IEEE VTC, Sept. 2008.

[21] R. Müllner, C. F. Ball, K. Ivanov, J. Lienhart, and P. Hric, "Contrasting open-loop and closed-loop power control performance in UTRAN LTE uplink by UE trace analysis," in Proc. IEEE ICC, Dresden, Germany, June 2009.

[22] M. Boussif, C. Rosa, J. Wigard, and R. Müllner, "Load adaptive power control in LTE uplink," in Proc. European Wireless Conf., Lucca, Italy, Apr. 2010, pp. 288–293.

[23] A. Karaer, Ö. Bulakci, S. Redana, B. Raaf, and J. Hämäläinen, "Uplink performance optimization in relay enhanced LTE-Advanced networks," in Proc. IEEE PIMRC, Sept. 2009, pp. 360–364.

[24] Ö. Bulakci, S. Redana, B. Raaf, and J. Hämäläinen, "System optimization in relay enhanced LTE-advanced networks via uplink power control," in Proc. IEEE VTC, May 2010.

[25] 3GPP Technical Specification TS 36.300. (2011, June). Overall description, stage 2. v.10.4.0. [Online]. Available: http://www.3gpp.org

[26] 3GPP Technical Specification TS 36.213. (2009, Dec). Evolved universal terrestrial radio access (E-UTRA) physical layer procedures (Release 8), v.8.5.0. [Online]. Available: http://www.3gpp.org

[27] 3GPP Technical Specification TS 36.101. (2008, Dec). Evolved universal terrestrial radio access (E-UTRA): User equipment (UE) radio transmission and reception (Release 8), v.8.4.0. [Online]. Available: http://www.3gpp.org

[28] H. Holma and A. Toskala, LTE for UMTS – OFDMA and SC-FDMA Based Radio Access. Wiley, 2009.

[29] D. Laselva, F. Capozzi, F. Frederiksen, K. I. Pedersen, J. Wigard, and I.

Z. Kovacs, "On the impact of realistic control channel constraints on QoS provisioning in UTRAN LTE," in *Proc. IEEE VTC*, Sept. 2009.

[30] I. Viering, A. Lobinger, and S. Stefanski, "Efficient uplink modeling for dynamic system-level simulations of cellular and mobile networks," *EURASIP J. Wireless Commun. Netw.*, 2010.

[31] F. D. Calabrese, C. Rosa, M. Anas, P. H. Michaelsen, K. I. Pedersen, and P. E. Mogensen, "Adaptive transmission bandwidth based packet scheduling for LTE uplink," in *Proc. IEEE VTC*, Canada, Sept. 2008.

[32] Ö. Bulakci, A. Bou Saleh, Z. Ren, S. Redana, B. Raaf, and J. Hämäläinen, "Two-step resource sharing and uplink power control optimization in LTE-advanced relay networks," in *Proc. IEEE MC-SS*, Germany, May 2011.

[33] A. Bou Saleh, Ö. Bulakci, Z. Ren, S. Redana, B. Raaf, and J. Hämäläinen, "Resource sharing in relay-enhanced 4G networks–downlink performance evaluation," in *Proc. IEEE European Wireless Conf.*, Austria, Apr. 2011.

[34] Ö. Bulakci, S. Redana, B. Raaf, and J. Hämäläinen, "Performance enhancement in LTE-advanced relay networks via relay site planning," in *Proc. IEEE VTC*, May 2010.

[35] P. Mogensen, N. Wei, I. Z. Kovacs, F. Frederiksen, A. Pokhariyal, K. I. Pedersen, T. Kolding, K. Hugl, and M. Kuusela, "LTE capacity compared to the Shannon bound," in *Proc. IEEE VTC*, Dublin, Ireland, Apr. 2007, pp. 1234–1238.

[36] 3GPP TR 36.942. (2008, Sept). Evolved universal terrestrial radio access (E-UTRA): Radio frequency (RF) system scenarios, v.8.0.0. [Online]. Available: http://www.3gpp.org

Bernhard Raaf received his Diploma degree on Physics in 1990 from Technical University of Munich, Germany, working on Radar measurements on auroral arcs at the Max Planck Institute for Extraterrestrial Physics. He then joined Siemens AG Mobile Phones in 1991 where he worked on ASIC design, software design and implementation, system optimizations, design reviews, conformance testing, and GSM type approval. Since 1997, he is leading research activities for standardization of UMTS with focus on system concept enhancements of UMTS, HSDPA, HSUPA, LTE, and recently LTE-Advanced. He is now Principal Engineer in the Radio Systems department within the research unit of Nokia Siemens Networks. He published 23 papers in journals and conferences, including Best Paper Award on IEEE VTC 2004-Fall, filed some 250 patent applications and holds some 90 granted patents, several of which are essential.

Jyri Hämäläinen received his M.Sc. and Ph.D. degrees from University of Oulu, Finland, in 1992 and 1998, respectively. From 1999 to the end of 2007, he was with Nokia and Nokia Siemens Networks where he worked on various aspects of mobile communication systems. Since 2008, he has been a Professor in Aalto University, Department of Communications and Networking. His current research interests include multi-antenna transmission and reception techniques, scheduling, relays, femtocells, and design and analysis of wireless networks in general. He is author or co-author of round 100 scientific publications and 30 US patents or patent applications.

Ömer Bulakci received his B.Sc. degree with High Honor in Electrical and Electronics Engineering in 2006 from Middle East Technical University in Turkey, and his M.Sc. degree with Distinction in Communications Engineering in 2008 from Technical University of Munich in Germany. In 2009, he joined Nokia Siemens Networks as a Ph.D. candidate of Aalto University School of Electrical Engineering, Finland. His current research interests are in wireless communications specifically focused on radio resource management in multi-hop relay networks.

Simone Redana is the Senior Research Engineer in the Radio Research unit of Nokia Siemens Networks, heading research and standardization projects on relaying in LTE-Advanced. He received his Ph.D. degree in Telecommunication Engineering from Politecnico di Milano, Italy in 2005. In 2005 and 2006, he was with Azcom Technology as Consultant for Siemens Communication. In 2006, he joined Siemens Communication in Milan, Italy, which merged in 2007 with Nokia Networks to become Nokia Siemens Networks. Since 2008, he is with Nokia Siemens Networks in Munich, Germany. He contributed to the EU WINNER II project, to the Eureka Celtic project WINNER+ and to the EU ARTIST4G project, leading the work package on advanced relay concept design. He is currently contributing to the 3GPP RAN standardization of relaying in Release 10 and beyond as well as being involved in the business case analysis for relays.